# A Strategy for Improving Reliability of Field-Oriented Controlled Induction Motor Drives

Tian-Hua Liu, *Member, IEEE,* Jen-Ren Fu, *Student Member, IEEE,* and Thomas A. Lipo, *Fellow, IEEE*

*Abstract*— **Although design of induction motor drives employing field-oriented control has reached a relatively mature state, relatively little effort has been expended on improving the reliability of these drives. In this paper a new, improved induction motor drive topology and control strategy is proposed that allows for continuous, disturbance free operation of the drive even with complete loss of one leg of the inverter or motor phase. A complete analysis and computer simulation of this new control and circuit concept is included.**

## I. Introduction

In the past several decades substantial progress has been made in the development of ac motor drives using both hard switched dc link and resonant-link schemes that utilize high speed switching devices such as fast recovery bipolar junction transistors, insulated gate bipolar transistors (IGBT's) and GTO's. Switching losses of hard switched converters (dc voltage link converters) have also improved dramatically due to the substantially reduced turn off time of third generation IGBT's. Also, control strategies, particularly field-oriented control strategies, have greatly improved the performance of ac motor drives. These control strategies utilize almost exclusively pulse width modulated (PWM) switching strategies that exploit the low switching loss capability of these converters and seek to produce a precisely controlled current to the windings of the motor. In effect, the controller serves to convert the dc/ac inverter from a voltage to a current source thereby overcoming many (but not all) of the inaccuracies involved in induction motor torque control.

While current regulation has greatly improved the torque response of ac drives, the use of this principle as a means of avoiding problems during system faults is relatively unappreciated. One of the most common types of faults, is the loss of a transistor in one of the legs of the inverter, or alternatively, the loss of one of the phases of the motor. In this case one of the motor phases is suddenly open-circuited, essentially single phasing the motor, resulting in a loss of field orientation and in high pulsating torques. Braking of the motor is then typically initiated using one of the following strategies: 1) friction braking, 2) dc current injection into the stator of the machine, 3) capacitive self-excitation braking, or 4) magnetic braking by shorting two or three stator leads [1]–[3] or combinations of these braking schemes. In all cases, these strategies involve expensive mechanical devices such as friction brakes or mechanical contactors to initiate the braking process.

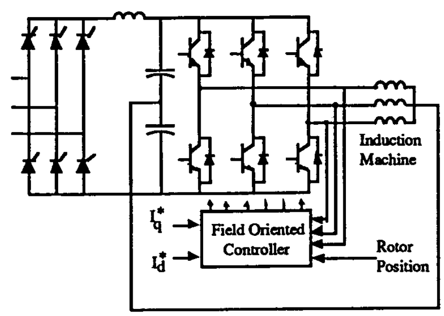


Fig. 1. Induction motor drive with machine neutral fed back to dc bus midpoint.

The cost and complications arising during emergency braking can be eliminated by considering the drive circuit shown in Fig. 1. It can be noted that this topology differs from the standard ac drive topology only in that the neutral point of the motor is returned to the midpoint on the dc voltage link. The midpoint is created by simply splitting the capacitor bank into two equal sections. During normal operation the stator current is regulated in normal PWM fashion by the field-oriented controller. In this case, the current flowing in the neutral of the machine, connected to the midpoint of the dc link, is essentially zero with possibly a very small current flowing due to PWM operation of the inverter. In the event that a transistor fails open in the inverter, however, a new current control strategy can be initiated by the converter that preserves the torque at its original value or changes the torque to any desired value while eliminating the negative pulsating torque usually associated with operation with an open phase.

## II. Analysis

In order to illustrate the concept for control during a single phase open circuit it is useful to employ the principle of space phasors [4]. In particular, assume that at "$t = 0^-$" all three

Paper IPCSD 92-47, approved by the Industrial Drives Committee of the IEEE Industry Applications Society for presentation at the 1991 Annual Meeting of the IEEE Industry Applications Society, Dearborn, MI, September 28–October 4. Manuscript released for publication December 28, 1992.

T.-H. Liu is with the Department of Electrical Engineering of National Taiwan Institute of Technology, Taipei, Taiwan.

J.-R. Fu is with the Taiwan Power Company, Taipei, Taiwan.

T. A. Lipo is with the Department of Electrical and Computer Engineering, University of Wisconsin-Madison, Madison WI 53706.

IEEE Log Number 9212089.

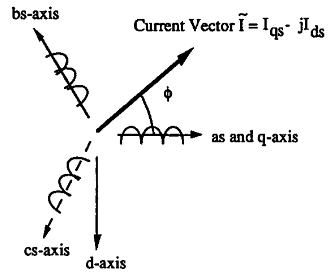


Fig. 2. Orientation of the current space vector just before one phase is open-circuited.

phases are excited normally and the current space phasor is located as shown in Fig. 2.

It is assumed that before any phase is open-circuited, the currents feeding the induction motor are regulated to be three balanced positive sequence sinusoidal currents, i.e.

$$\begin{aligned} I_{as} &= I\cos(\omega t + \phi) \\ I_{bs} &= I\cos(\omega t + \phi - 2\pi/3) \\ I_{cs} &= I\cos(\omega t + \phi + 2\pi/3). \end{aligned} \tag{1}$$

The rotating MMF generated by the armature currents is the sum of the MMF's caused by each of the three phases. Based on the three axes shown in Fig. 2, this MMF can be expressed by the complex vector

$$\begin{aligned} \text{MMF} &= \text{MMF}_a + \text{MMF}_b + \text{MMF}_c \\ &= NI_{as} + aNI_{bs} + a^2NI_{cs} \end{aligned} \tag{2}$$

where $a = 1\angle 120°$ and $N$ is the effective number of stator turns per phase. For balanced three-phase operation

$$\text{MMF} = \frac{3}{2}Fe^{j\theta} \tag{3}$$

$$= \frac{3}{2}F(\cos\theta + j\sin\theta) \tag{4}$$

where $F = NI$ and $\theta = (\omega t + \phi)$.

Assume that at any time $t$, the current in phase $b$ suddenly drops to zero. In this case, the rotating MMF will be the sum of $\text{MMF}_a$ and $\text{MMF}_c$ only, i.e.

$$\begin{aligned} \text{MMF}' &= NI'_{as} + a^2NI'_{cs} \\ &= NI'_{as} + NI'_{cs}\left(-\frac{1}{2} - j\frac{\sqrt{3}}{2}\right) \end{aligned} \tag{5}$$

where the prime indicates the new values of each variable after one phase is open-circuited.

The same MMF is maintained after phase $b$ is open-circuited by setting (4) equal to (5) and then solving for real and imaginary parts separately

$$\frac{3}{2}F\cos\theta = NI'_{as} - \frac{1}{2}NI'_{cs} \tag{6}$$

$$\frac{3}{2}F\sin\theta = -\frac{\sqrt{3}}{2}NI'_{cs}. \tag{7}$$

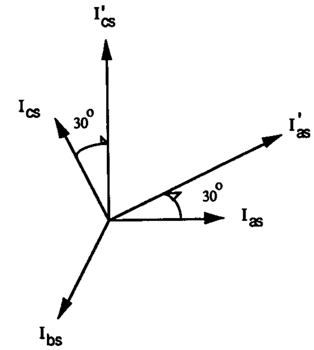


Fig. 3. Phasor relationships before and after phase $b$ is open-circuited.

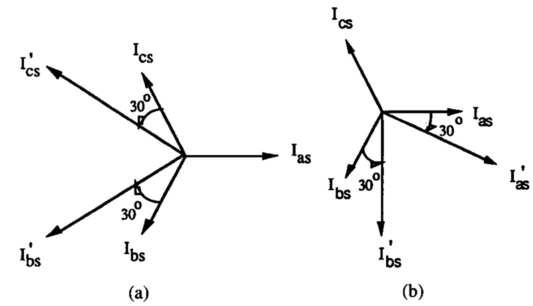


Fig. 4. Phasor relationships required for a unaffected operation when (a) phase $a$ is open-circuited and (b) phase $c$ is open-circuited.

From these two equations, it can be determined that

$$\begin{aligned} I'_{cs} &= -\sqrt{3}I\sin\theta \\ I'_{as} &= \frac{3}{2}I(\cos\theta - \frac{1}{\sqrt{3}}\sin\theta) \end{aligned} \tag{8}$$

or, equivalently

$$\begin{aligned} I'_{as} &= \sqrt{3}I\cos(\omega t + \phi + \pi/6) \\ I'_{cs} &= \sqrt{3}I\cos(\omega t + \phi + \pi/2). \end{aligned} \tag{9}$$

Hence, if phase $b$ is open-circuited, "disturbance-free" control is possible if phase $a$ current is regulated to advance by 30° and phase $c$ current regulated to be retarded 30°. Both phase $a$ and phase $c$ current magnitude must also be increased to $\sqrt{3}$ times their previous value. Fig. 3 shows the phasor relationships before and after phase $b$ is suddenly open-circuited.

The same analysis can be applied to the cases of phase a or phase b being open-circuited. If phase a is open-circuited, then control of the remaining two currents after the open circuit should be

$$I'_{bs} = \sqrt{3}I\cos(\omega t + \phi - 5\pi/6) \tag{10}$$

$$I'_{cs} = \sqrt{3}I\cos(\omega t + \phi + 5\pi/6). \tag{11}$$

If phase $c$ is open-circuited

$$I'_{as} = \sqrt{3}I\cos(\omega t + \phi - \pi/6) \tag{12}$$

$$I'_{bs} = \sqrt{3}I\cos(\omega t + \phi - \pi/2). \tag{13}$$

Fig. 4 shows the phasor relationship before and after phases $a$ and $c$ are open-circuited. In any of the above three cases, it is noted that after the opening of one phase the remaining two phases should be regulated to a magnitude of $\sqrt{3}$ times of their original value and phase-shifted 60° with respect to each other. The new phase angle is accomplished by regulating one phase to jump forward 30° and the other phase to jump backward 30° with respect to their positions before the open circuit.

Fig. 5 shows an idealized example of a typical scenario in that the motor phase $c$ is open-circuited at $t = 0$ for the special case in which $f = 0$. The only torque transient to be expected is the result of the $di/dt$ limit of the inverter imposed by the maximum dc link voltage.

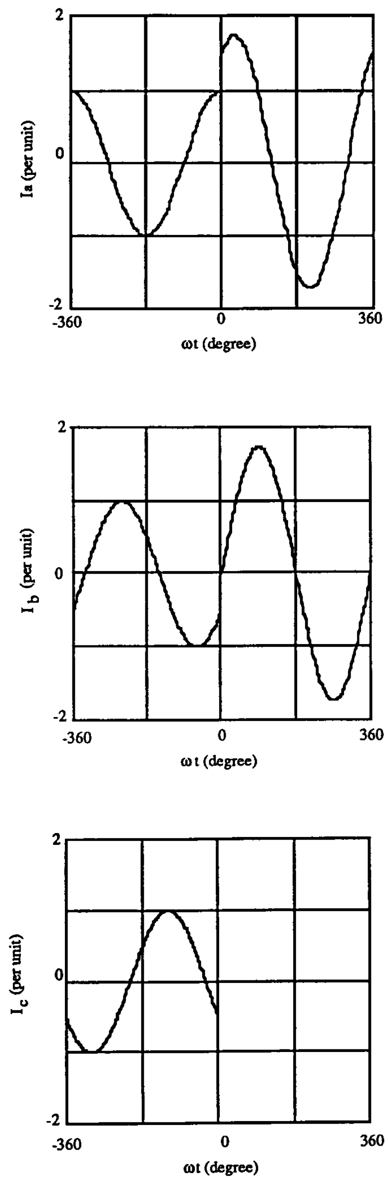


Fig. 5. Phase currents before and after a sudden open circuit of phase $c$, which results in the same instantaneous torque and notorque transient.

## III. Computer Simulation

### A. Simulation Model

To verify the aforementioned principles, a simple computer model for field-oriented controlled induction motor was established. In this model, indirect field orientation was implemented based on the slip relationship for field orientation [5]

$$s\omega_e = \frac{R_r}{L_r}\frac{I_{qs}}{I_{ds}}. \tag{14}$$

A speed control loop with a PI controller is used to control the motor speed. The PI controller compares the preset speed setting to the rotor speed signal and generates a torque command, i.e., $I_{qs}^*$. The flux command $I_{ds}^*$ is assumed to be constant in the simulation. The field angle $\theta_{rf}$, which is required to transform the $d$-$q$ axis commands to $a$-$b$-$c$ axis commands, is generated by summing the rotor-position signal and the slip-position signal. The rotor-position signal is obtained directly from the integration of the rotor speed. Using the calculated value of $\theta_{rf}$, the current commands in the $d$-$q$ axis $I_{qs}^*$ and $I_{ds}^*$ are transformed to current commands in the $a$-$b$-$c$ axis $I_{as}^*, I_{bs}^*$ and $I_{cs}^*$. The commanded currents $I_{as}^*$, $I_{bs}^*$, and $I_{cs}^*$ are then compared to the motor stator currents $I_{as}$, $I_{bs}$, and $I_{cs}$, which are generated from the dynamic model of the induction motor. Three current-regulated delta modulators operated under a specified sampling frequency are used to generate the switching pattern for each phase. These switching patterns are then used to control the switches of the current regulated PWM inverter.

The following motor parameters are used in the simulation: $L_s = 0.07131$ h, $L_r = 0.07131$ h, $L_m = 0.06931$ h, $R_s = 0.435\Omega$, $R_r = 0.816\Omega$, $V_{dc} = 198$ V, $K_I = 0.01$, $K_P = 0.1$, Commanded speed = 1000 rpm, Switching frequency = 5 kHz.

The dynamic model of the induction motor is based on Stanley's equations. In general, the simulation of a one-phase open-circuited condition can be achieved by two means. The first method employs the use of the induced voltage in the open winding [6]. The voltage appears across the open winding can be determined by the mutual inductance, rotor leakage inductance and the rotor rotating flux. The other method assumes zero current in the open phase as a constraint. Substituting this constraint into Stanley's equations, a second set of dynamic equations dedicated to one-phase open-circuit operation can be derived.

### B. Simulation Results

Both the simulation of motor starting and normal operation with and without load have been implemented. In all cases, one phase current is assumed to drop to zero suddenly while the remaining two phases are regulated to the new magnitude and phase angles required to maintain the same MMF as discussed

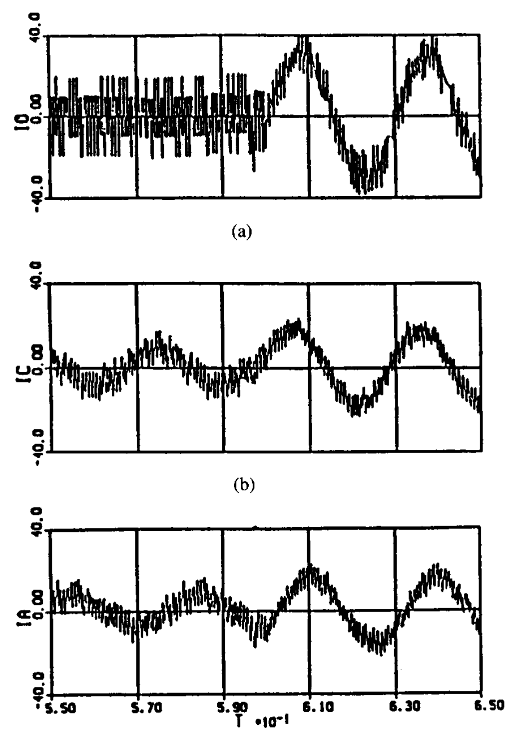

Fig. 6. Current variation after phase b is open-circuited (a) $I_{os}$, (b) $I_{cs}$, (c) $I_{as}$.

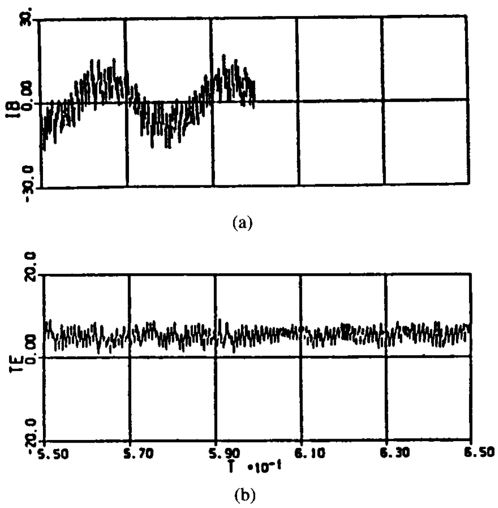

Fig. 7. Torque variation after phase b is open-circuited. (a) $I_{bs}$. (b) Torque.

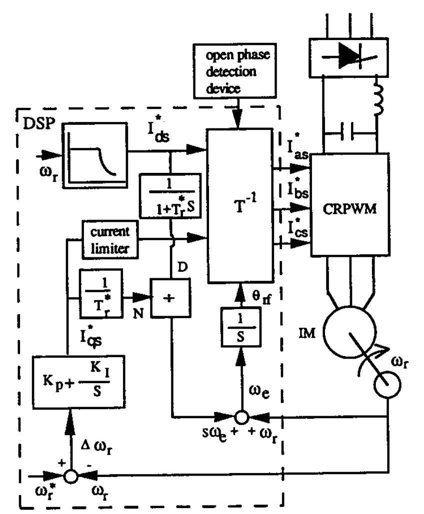


Fig. 8. System control block diagram incorporating open-circuit contingency control.

in Section II. Figs. 6 and 7 are the simulation results for the case where phase b is suddenly open-circuited.

Note from Fig. 6 that under this type of unbalanced operation, the neutral current $I_{os}$ is no longer zero. Instead, it becomes the sum of $I_{as}$ and $I_{cs}$ and is three times the value of the original operating line current before the open circuit. From Fig. 7 it can be noted that although the phase b current drops to zero at $t = 0.6$ s, the torque is almost unaffected.

## IV. Control System Block Diagram

The system of Fig. 8 shows one method for implementing the proposed scheme by modifying the indirect field-oriented control strategy. The basic concept is same as the simulation model described in Section III-A. In addition, a device to sense the operating condition is required in order to implement a control scheme change. This device should have the ability not only to detect the open circuit but also to identify the different phases so that the system can switch to the appropriate control scheme accordingly. The $a$-$b$-$c$ axis current commands are obtained from the $d$-$q$ to $a$-$b$-$c$ axis transformation. For example, for normal operation, the current commands are

$$I_{as}^* = I_{qs}^* \cos\theta + I_{ds}^* \sin\theta \quad (15)$$

$$I_{bs}^* = I_{qs}^* \cos(\theta - 2\pi/3) + I_{ds}^* \sin(\theta - 2\pi/3) \quad (16)$$

$$I_{cs}^* = I_{qs}^* \cos(\theta + 2\pi/3) + I_{ds}^* \sin(\theta + 2\pi/3). \quad (17)$$

When phase $b$ is open, the current commands should become

$$I_{as}^* = \sqrt{3}[I_{qs}^* \cos(\theta + \pi/6) + I_{ds}^* \sin(\theta + \pi/6)] \quad (18)$$

$$I_{cs}^* = \sqrt{3}[-I_{qs}^* \sin\theta + I_{ds}^* \cos\theta]. \quad (19)$$

It is clear that the controller of the proposed system can readily take advantage of today's digital signal-processing technology. As shown in Fig. 8, continuous control can be transformed to the discrete domain by using a DSP. The digital controller provides not only a highly accurate but also drift-free control. The three control schemes required for the different open-circuit operations can be pre-programmed and stored in the memory of the digital signal processor. The main program is then interrupted to execute the contingency control as soon as an open-circuit signal is detected.

For proper two-phase operation, it is apparent that the capacitor midpoint voltage should be maintained at one half of

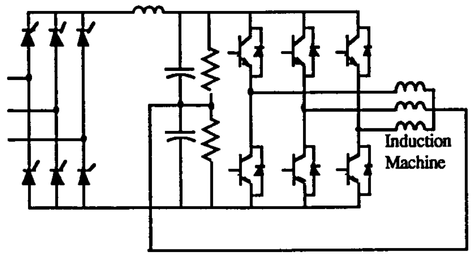


Fig. 9. Use of a pair of resistors to force voltage sharing across the dc link capacitors.

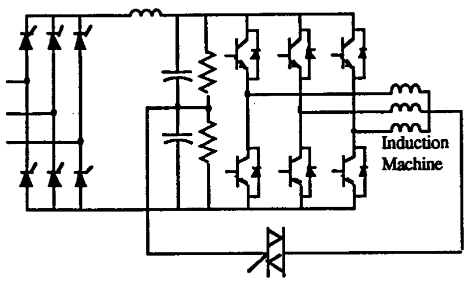


Fig. 10. Use of a triac to block the neutral current during normal operation.

the dc bus voltage. To prevent the capacitor midpoint voltage from drifting from this desired voltage, the following three control methods can be considered:

a) A pair of small resistors can be used to help stabilize the drift as shown in Fig. 9. In this case some extra losses are clearly incurred. However, in most cases the added losses can be considered as negligible.
b) It can be noted in Fig. 8 that the neutral current is not zero but carries a high frequency switching current with zero average value due to the PWM inverter. A triac can be connected between the capacitor midpoint and the motor neutral point to eliminate this current. During normal operation, the triac is blocked, so no current will flow to unbalance the charge to the capacitors. The triac is only triggered "on" when the one-phase open signal is detected and a two-phase operation is required. Fig. 10 shows a sketch of this control method.
c) Introduce a flux or torque command regulator to manipulate the motor-current commands so that the capacitor midpoint voltage will be regulated and will not deviate much from the desired value. Fig. 11 shows the control block diagram of this method using flux as the correcting signal. The variation of the flux command may result in the torque variation. However, this variation is considered not to be significant. The speed change as a result of flux command change will finally be compensated through the speed feedback control loop.

## V. Further Simulations

One of the important factors in the practical implementation of this control strategy is the selection of the capacitor size. Under unbalanced two-phase operation, the neutral current

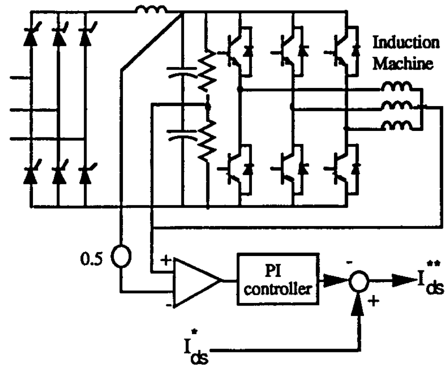


Fig. 11. Flux command control method.

becomes three times that of the line current required for normal operation so that the link voltage could be subjected to severe pulsations in amplitude. To simplify the evaluation, it is assumed that stator currents are regulated exactly to be a sinusoidal waveform so that the neutral current can be considered as a current source charging the capacitors. By comparing the impedances of the capacitor and the damping resistor, one can conclude that most of the current will flow through the capacitor. Hence, the voltage variation across the capacitors is estimated as

$$\Delta V = \frac{I_{os}}{2j\omega_e C} \tag{20}$$

where $I_{os}$ neutral current
$\omega_e$ electrical frequency
$C$ dc link capacitance.

Hence, the capacitor selection strongly depends on the operating current, frequency, and the voltage-variation tolerance. A rough estimate for the case simulated in this paper, to keep the voltage variation less than 10% of the dc voltage, a capacitor of about 0.004 F is required. However, for higher load operation or more strict voltage-variation tolerance, a higher capacitor size is required accordingly.

Fig. 12 shows a modified simulation in which the effects of the finite link capacitor are incorporated into the computer model. In particular, the value of the dc link capacitance was chosen as 10 000 $\mu$F. Method b), above, was used to prevent link voltage drift. That is, a triac is triggered to tie the motor neutral back to the dc voltage midpoint only when an open circuit is detected. Note that the dc link voltage now sustains a moderate ripple voltage. However, examination of the motor torque verifies that the control is not affected.

In Figs. 13 and 14, operation with the resistive damping circuit and with the flux command regulator are portrayed by means of simulation. Considering both the damping effect and power dissipation, values of 1000 $\Omega$ were used for the two damping resistors. Using this selection, with the capacitor and the dc voltage used in the simulation, the damping time constant is 10 s and power dissipation is 20 W. Again it can

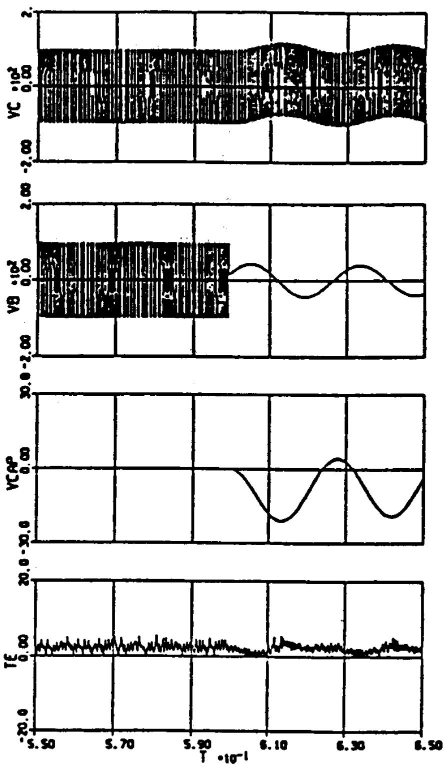

Fig. 12. Opening of phase $b$ using the circuit of Fig. 10. Traces from top to bottom are: Phase $c$ voltage; phase $b$ voltage; dc linkmidpoint voltage; electromagnetic torque.

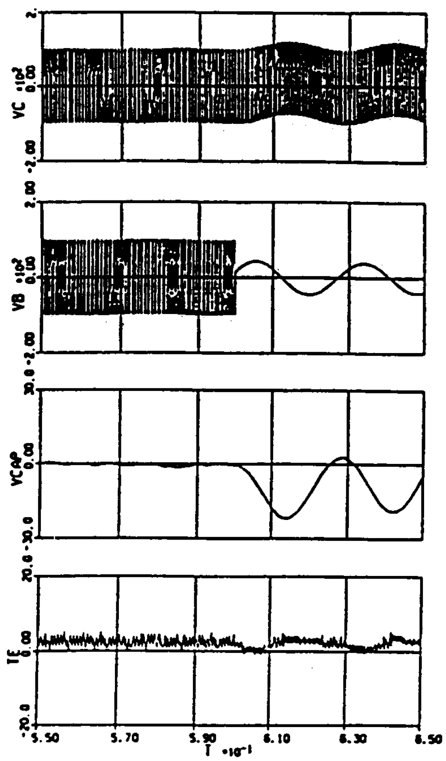

Fig. 13. Opening of phase $b$ using the circuit of Fig. 9. Traces from top to bottom are: phase $c$ voltage, phase $b$ voltage, dc linkmidpoint voltage, electromagnetic torque.

be noted that the currents are well-regulated and that drift of the dc link midpoint voltage is well-damped both before and after the open circuit occurs.

## VI. Experimental Results

To verify the control strategy discussed in Section IV, a 7.5 HP General Electric induction motor and Motorola DSP 56 000 Application Development System has been used to implement the control block diagram shown in Fig. 8. Also, an Emerson adjustable frequency ac drive was modified to accept the switching pattern signals generated from a digital signal processor (DSP). An encoder attached to the motor shaft provides pulse signals so that the motor speed can be measured by counting the pulses. Three current sensors, one for each phase, provide analog current signals. By means of an analog-to-digital card, these analog signals were transformed into digital signals and were utilized in a DSP. A neutral line was connected between the motor neutral and the dc midpoint so that the current of the remaining two phases can be individually controlled after one phase is open-circuited.

A pair of back-to-back connected SCR's were used to switch off the motor phase current. The current was interrupted at a zero crossing in the same manner as used in the simulation study, Section III. The current was interrupted at a zero crossing to prevent possible high induced voltages due to the high $di/dt$ of the inductive motor current. In practice an open circuit can occur at any current level and an electrical arc will temporarily accompany an open circuit fault. However, this transient will not affect the long-term operation of the proposed control strategy. Simple RC snubber circuits were also used to protect the SCR's in the neutral. A pair of resistors are used to help stabilize the drift of dc midpoint voltage, as shown in the control scheme of Fig. 9. The capacitance and resistor used were 10 000 $\mu$F and 750 ohms, respectively.

The DSP control-block diagram is shown in Fig. 15. The DSP was programmed to begin execution of the main program from program memory address location 100 (hexadecimal). First, to prevent the motor from conducting, a disable signal is sent to disable the PWM operation. The DSP then begins to obtain information regarding the rotor initial position and calculates the zero offset of the three current sensors. After this interval, the initial values of the state variables are loaded. When all these tasks are completed, the main program jumps to a subroutine to obtain the initial switching patterns. The initial switching patterns are obtained by assuming a constant torque command and flux command. This process is repeated about 1000 times so that the machine speed decreases somewhat before the controller is again put into a field-oriented control condition. Before the DSP begins to perform field-oriented control, the timer

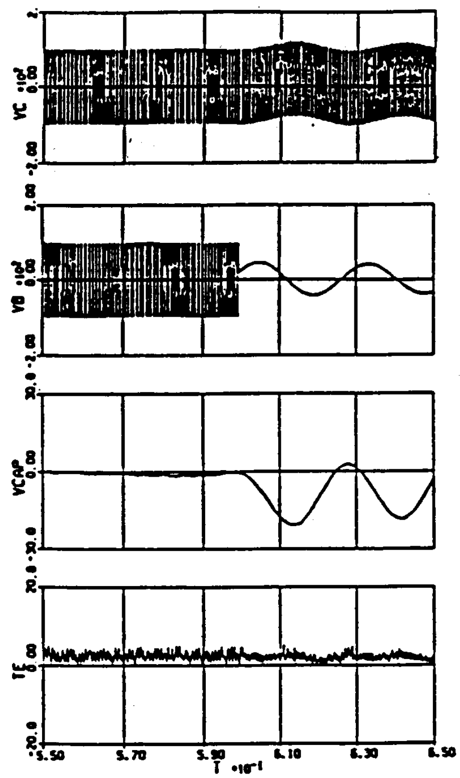


Fig. 14. Opening of phase $b$ using the circuit of Fig. 11. Tracesfrom top to bottom are: phase $c$ voltage, phase $b$ voltage, dc linkmidpoint voltage, electromagnetic torque.

in the DSP must be set to allow an interrupt occur. The timer was, in this case, set to limit the maximum switching frequency of the delta modulated PWM to be less than the maximum allowable hard switching frequency of the switching devices.

During field-orientation control, $I_{qs}^*$ is calculated in the synchronous frame from the speed error and a PI controller as discussed in Section IV. During each calculating cycle, an open-circuit determination logic is performed to decide whether or not an open-circuit fault has occurred. If it is in the normal operation mode, $I_{qs}^*$ and $I_{ds}^*$ are transformed into $I_{as}^*$, $I_{bs}^*$ and $I_{cs}^*$. If one phase is open-circuited, $I_{qs}^*$, and $I_{ds}^*$ are transformed by the theory introduced in this paper into current commands for the remaining two healthy phases. These current commands then compared to the actual current signals and generate the PWM switching patterns. In the open-circuit determination logic, special consideration must be given to prevent mistaking a current zero crossing as an open-circuit fault. Normally, there is a minimum time required to confirm an open-circuit fault exists. This minimum time is determined by the current magnitude, frequency, and random noise level. The time required to justify an open-circuit fault is then converted to a number consistent with the program sampling frequency so that DSP can count the open-circuit time by means of clock cycles. A hysteresis CRPWM control scheme

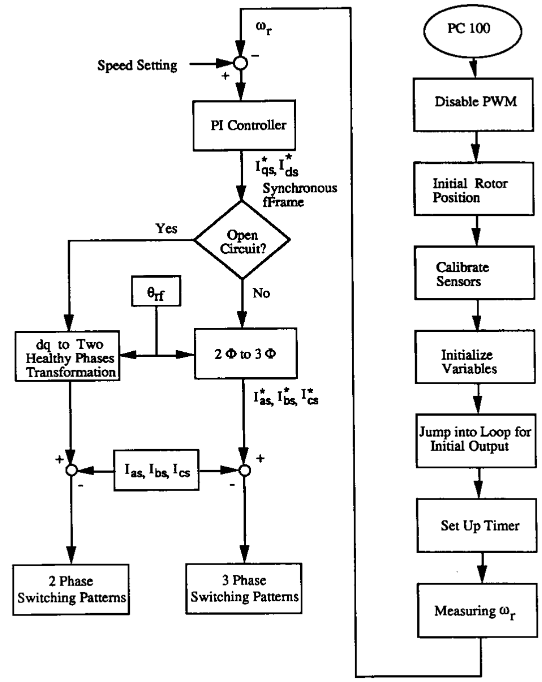


Fig. 15. DSP control block diagram.

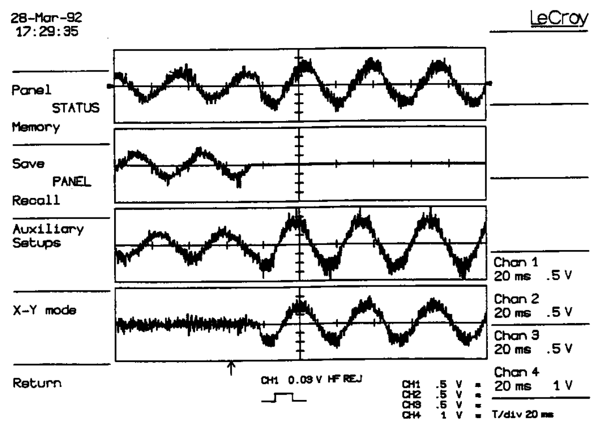


Fig. 16. Current waveforms of actual system during loss of a phase. a) Phase current $a$, b) phase current $b$, c) phase current $c$, d) motor neutral current.

was implemented to maintain the current at the desired value.

Fig. 16 shows the results for the experimental system in which phase $b$ is open-circuited by suddenly turning off the transistor switches corresponding to this phase. A substantial flow of high-frequency current in the motor neutral can be observed before the open circuit occurs. Clearly, this current can be reduced by either increasing the modulation frequency or by increase in the zero sequence inductance either by motor design or by physically inserting a small inductor in the motor neutral. In the practical system, the PWM frequency was limited at about 5 kHz.

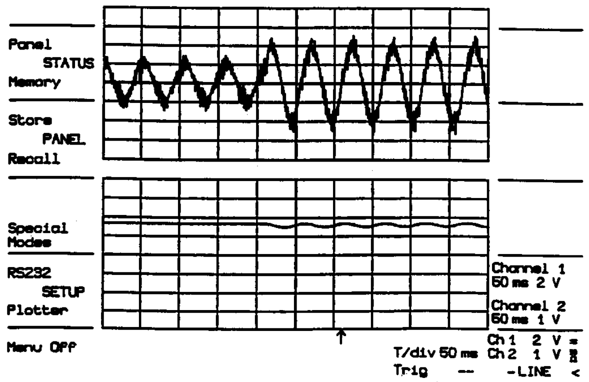


Fig. 17. Current and dc midpoint voltage waveforms of actual system during loss of a phase. a) Phase current $a$, b) dc midpoint voltage.

Fig. 17 shows the dc midpoint voltage variation after one phase is open-circuited. The data was taken with the motor driving a two-horsepower load.

## VII. Conclusion

This paper has reported the theory concerning a new principle of protection as well as the possibility of continuous operation under conditions where one phase is open-circuited. In particular, this paper introduces a new control strategy to implement this principle. A detailed digital computer simulation is used to verify the correctness of the theory. The limitations imposed by center tapping the dc link supply are discussed and the potential impact on capacitor selection due to the ac currents that now must flow in the link capacitors is evaluated. A proposed control scheme to implement this control strategy and the experimental results were also presented.

It is important to emphasize that *no negative sequence currents are produced by this choice of stator currents*, Hence, there are no pulsating torques created and the torque is undisturbed even though the current in one of the phases has been interrupted. Clearly, this control strategy not only allows for "disturbance-free" operation of the motor but affords a significant cost reduction compared to previous schemes that used contactors, extra capacitors, and friction brakes to obtain the same degree of protection. It is important to also note that the machine remains completely *field-oriented* and that the motor can continue to operate on only *two phases* as long as necessary to complete a required operation or can immediately enter the regenerative mode for the purpose of stopping the motor as quickly as possible. In contrast to previous schemes using a dc current or with shorted windings, in which the braking torque strategy was to "take whatever you can get," this braking action is done under precise field-oriented control.

It can be readily shown that the stator copper loss is unfortunately doubled under unbalanced two-phase operation (rotor copper loss is unaffected). However, it is apparent that the motor can continue to operate indefinitely with one-third of rated torque. This may be useful for completing, for example, a machining operation under a lower feed rate than normal before shutting down for repair. Furthermore, shut down is accomplished under field-oriented control in which the braking torque can be carefully regulated, eliminating the possibility of broken tools, shafts, etc. Conversely, the motor and converter can be sized to accommodate the extra losses incurred by unbalanced two-phase operation so that the motor and converter can then operate indefinitely under full load if the inverter frequency is sufficiently high to limit the ripple current to an acceptable value. Such considerations could be extremely important in the case of critical loads such as a cooling pump in a nuclear power plant. If continuous two-phase operation is attempted it should be cautioned, however, that the unsymmetrical concentration of heat around the stator periphery could cause distortion of the stator laminations, without proper attention to bracing. Finally, perhaps it is also useful to mention that this new control strategy can be implemented for *any* type of ac drive including induction, wound field synchronous, synchronous reluctance, and permanent magnet motor drives.

## References

[1] S. A. Choudhury and S. P. Hastings, "Dynamic braking of induction motors," *AEI Eng.*, July/Aug. pp. 186–192, 1964.
[2] S. S. Murthy, G. J. Berg, C. S. Jha, and A. K. Tandon, "A novel method of multistage dynamic braking of three phase induction motors," in *Proc. IEEE Int. Semiconductor Power Converter Conf.*, May 1982, pp. 287–294.
[3] G. A. Kaufman and M. J. Kocher, "Fail-safe dynamic brake for three phase induction machines," *IEEE Trans. Ind. Applicat.*, vol. IA-20, no. 5, Sept./Oct. 1984, pp. 1229–1237.
[4] W. Leonhard, "Control of electrical drives." New York: Springer-Verlag, 1985.
[5] T. A. Lipo and D. W. Novotny, "Dynamics and control of ac drives," Univ. Wisconsin-Madison (text notes), 1991.
[6] P. C. Krause and C. H. Thomas, "Simulation of symmetrical induction machinery," *IEEE Trans. Power App. Syst.*, vol. PAS-84, no. 11, pp. 1038–1053, Nov. 1965.

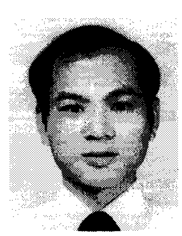

**Tian-Hua Liu** (S'85–M'89) was born in Tao Yuan, Taiwan, Republic of China, on November 26, 1953. He received the B.S., M.S., and Ph.D. degrees in electrical engineering from National Taiwan Institute of Technology, Taipei, Taiwan, in 1980, 1982, and 1989, respectively.

From 1984 to July 1989, he was an Instructor in the Department of Electrical Engineering, National Taiwan Institute of Technology. He was a Visiting Professor in the Department of Electrical and Computer Engineering at the University of Wisconsin–Madison, from 1990 to 1991. Since August 1989, he has been an Associate Professor in the Department of Electrical Engineering, National Taiwan Institute of Technology. His research interests include motor controls, power electronics, and microprocessor-based control systems.

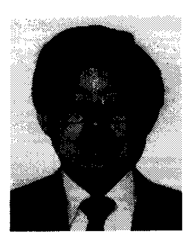

**Jen-Ren Fu** (S'91) received the B.S. degree in electrical engineering in 1973 from the National Cheng-Kung University, Tainan, Taiwan. He received the master of engineering degree in energy technology from the Asia Institute of Technology, Bangkok, Thailand, in 1988. He received the Ph.D. from the Electrical and Computer Engineering Department of the University of Wisconsin–Madison in 1993.

He joined the Taiwan Power Company in 1975, where he has been engaged in the Engineered Safety Feature design for nuclear power plants and the Equipment Qualification of the safety-related systems. His current research interests include simulation of electric machines and drives, microprocessor-based real-time control, modeling of global energy consumption, and cogeneration systems.

Mr. Fu is a Registered Professional Engineer in Taiwan. He is a member of the Chinese Association of Energy Economics.

**Thomas A. Lipo** (M'64–SM'71–F'87) is a native of Milwaukee, WI. He received the B.E.E. and M.S.E.E. degrees from Marquette University, Milwaukee, WI, in 1962 and 1964, and the Ph.D. degree in electrical engineering from the University of Wisconsin in 1968.

From 1969 to 1979, he was an electrical engineer in the Power Electronics Laboratory of Corporate Research and Development of the General Electric Company, Schenectady, NY. He became Professor of Electrical Engineering at Purdue University in 1979, and in 1981, he joined the University of Wisconsin in the same capacity, where he is presently the W. W. Grainger Professor of Power Electronics and Electrical Machines.

Dr. Lipo has maintained a deep research interest in power electronics and ac drives for over 25 years. He has received 11 patents and has 13 IEEE prize paper awards for his work, including corecipient of the Best Paper Award in the IEEE TRANSACTIONS ON INDUSTRY APPLICATIONS for the year 1984. In 1986, he received the Outstanding Achievement Award from the IEEE Industry Applications Society for his contributions to the field of ac drives, and in 1990, he received the William E. Newell Award of the IEEE Power Electronics Society for contributions to the field of power electronics.